Supplemental Methods

General motor execution

General motor execution was measured after the stimulation but before MSL training using a random serial reaction time task (SRTT[1]), implemented in Matlab. This task was also performed inside the scanner but without acquiring the corresponding fMRI data. Participants saw eight squares on the screen, each representing one of the eight keys of the specifically designed keyboard and one of the 8 fingers (except thumbs). Green outlines of the squares indicated practice and red outlines rest blocks. For each green filled square appearing on the screen during the practice blocks, the key corresponding to the square's location had to be pressed as rapidly as possible. The following square was filled green after a key press (response-stimulus interval=0ms) according to a pseudorandom order and independent of the correctness of the previous key press. After 48 key presses the squares automatically turned red, indicating a rest block. During rest blocks (duration: 10s), participants were asked to look at the screen and to not move their fingers. The task included four practice blocks. During the performance of the SRTT, the timing and number of key presses was documented, and performance was measured in terms of speed (mean time to perform a correct key press per block) and accuracy (percentage of correct key presses per block). Repeated measures ANOVAs were conducted for speed as well as accuracy measures with blocks (4) as within-subject factor and group as between-subject factor (cTBS/iTBS/control), and the corresponding results are reported below.

Motor evoked potentials

Motor evoked potentials (MEPs) were measured with a belly-tendon EMG montage on the right flexor dorsal interosseous (FDI) muscle. Active motor threshold (aMT) was characterized during voluntary submaximal FDI contraction as the lowest intensity for which minimum 5/10 MEPs were distinguishable from background EMG[2,3]. Resting motor threshold (rMT) was defined with single pulse stimulation of the M1 hotspot as the lowest intensity at which at least 5/10 MEPs measured on the FDI were larger than 50μV. As readout of corticospinal excitability changes in M1, twenty-one MEPs at 120% rMT were measured at two timepoints, i.e., pre- and post-TBS. Due to technical issues, MEP measurements are missing for 2

participants (1 control, 1 cTBS). Additionally, due to experimental error or interruption of the stimulation procedure because of participants' discomfort, MEP data of 7 participants (2 control, 4 cTBS, 1 iTBS) include less than 21 MEPs (with a minimum of 16 MEPs). The first MEP of each timepoint was excluded as their amplitudes are usually higher than subsequent MEPs due to reflex or startle responses. MEPs smaller than 50μV were excluded from the analysis (11.07%) and all remaining MEPs were visually inspected, leading to additional exclusions of 17 MEPs (0.72%). Additionally, we performed an outlier analysis (3SD) on MEPs pre-TBS per participant, leading to no additional excluded MEPs. One participant was excluded from the MEP analyses due to background EMG noise (control group) and 6 additional participants (1 control, 2 cTBS, 3 iTBS) were excluded as they did not have enough remaining MEPs after the above-described exclusions (<10 MEPs left for pre- and/or post-TBS MEPs). MEPs of the remaining 60 participants (18 control, 21 cTBS, 21 iTBS) were averaged per timepoint and per individual (pre-TBS and post-TBS on experimental day 1, see Supplemental Figure S1) and entered into a repeated measures ANOVA with timepoint (pre-/ post-TBS) as within-subject factor and group (cTBS/iTBS/control) as between-subject factor. Additionally, changes in MEPs were calculated from pre- to post-TBS as the percentage of difference between timepoints and correlated with offline gains in performance using Pearson's correlation. Percent change in MEPs were also used as covariates in fMRI regression analyses.

Additional MR image acquisitions

During the baseline session we acquired additional T1 (TR/TE=8/3.8ms; voxel size=0.85×0.85×0.85mm^3; field of view=245×245×208.25mm^3; 245 sagittal slices, selective water excitation, bandwidth=299.3Hz) and T2 (TR/TE=2500/272ms; voxel size=0.85×0.85×0.85mm^3; field of view=245×245×190.4mm^3; 224 sagittal slices, bandwidth=876.8Hz) anatomical scans as well as RS fMRI data using an ascending gradient EPI pulse sequence for T2*-weighted images (TR=1000ms; TE=33ms; multiband factor 3; flip angle=80°; 42 transverse slices; interslice gap=0.5mm; voxel size=2.14×2.18×3mm^3; field of view=240×240×146.5mm^3; matrix=112×110; 300 dynamic scans) for each participant. During RS data acquisition, a dark screen (i.e., no visual stimuli) was presented and participants were instructed to remain still, close their eyes and to not think of anything in particular for the duration of the scan. The additional T1, T2 and RS data were not analyzed in the current study.

Individual DLPFC peak definitions

We ran – a posteriori – the same individual targeting pipeline as described in our earlier research[17] to test for the presence of individual peak of maximal connectivity with the striatal and hippocampal seeds in the 15mm sphere centered around the fixed coordinate stimulated in this study. To do so, we performed whole-brain FC analyses using the hippocampus and caudate nucleus (bilaterally, as defined anatomically according to the AAL brain atlas[18]) as seeds on the RS data acquired during the baseline session. For each individual and for each seed, the time-series across all voxels within the seed were averaged and Pearson correlation coefficients with all the voxels of the brain were computed. To ensure normality, each correlation coefficient was Fishers r-to-z transformed using the formula $z = \text{arctanh}(r)$. Statistical analyses were performed on the z-values and were based on comparisons of the correlation coefficients to a value of 0. Statistical probabilities were considered significant if surviving the false discovery rate (FDR) method for multiple comparisons ($p_{FDR}<0.05$). A conjunction analysis testing the "Conjunction Null Hypothesis" was performed between the hippocampal and striatal FDR-corrected connectivity Z-maps in each individual using the easythresh_conj function[19] rendering the conjunction map onto an average brain template provided by FSL (www.fmrib.ox.ac.uk/fsl, avg152T1) and thresholded at the highest Z score of both RSFC maps. The individual's TBS target was characterized as the coordinate with the maximum Z-value within a 15-mm radius sphere mask centered on the fixed coordinate stimulated in the current study. Results showed significant conjunction peaks within the DLPFC sphere in each individual (see Supplemental Figure S2).

Electric field modelling

We modelled the effects of active and control stimulation on (i) the MNI template and (ii) on a few exemplary individuals' anatomical scans to investigate the different electric fields (e-fields) of these conditions. As our TMS machine does not provide a readout of the dI/dt matching the exact %MSO (maximum stimulator output), we used an approximation based on unpublished data from our group. For the control stimulation, we used 14 000 000 A/s as dI/dt and for the active stimulation, we used 31 500 000 A/s as dI/dt in the newest version of the Brainsight software (2.5) with integrated SimNIBS to model electric fields. We used charm to segment the T1 scans for use in the SimNIBS projects and exported the DLPFC targets used

in the original Brainsight projects used for the application of TBS current study. The linear character of e-field distributions can be appreciated when comparing the simulations of the control and active TMS (see Supplemental Figure S3). However, it is worth noting that these types of simulations cannot take the effect of repetitive patterned TMS protocols into account.

Supplemental Results

Effect of prefrontal TBS on general motor execution

We investigated whether prefrontal stimulation altered general motor execution (GME) prior to initial training on experimental day 1 (see Figure 1A). While performance improved over the course of the performed random serial reaction time task (speed: $F_{(2.116,139.684)}$=30.933, η_p^2=0.319, p<0.001; accuracy: $F_{(3, 198)}$=2.42, η_p^2=0.035, p=0.067), neither performance speed (main effect of group: $F_{(2,66)}$=0.352, η_p^2=0.011, p=0.704; group by block interaction: $F_{(4.233,139.684)}$=0.606, η_p^2=0.18, p=0.668) nor performance accuracy (main effect of group: $F_{(2,66)}$=2.225, η_p^2=0.063, p=0.116; group by block interaction: $F_{(6,198)}$=0.544, η_p^2=0.016, p=0.774) differed among groups.

Effect of prefrontal TBS on performance accuracy during MSL training

Behavioral results show that performance accuracy (i.e., percentage of correct transitions) significantly improved across practice blocks during the MSL training session (training panel: blocks 1-20; main effect of block: $F_{(12.331,813.87)}$=1.811, η_p^2=0.027, p=0.041) similarly between groups (block by group interaction: $F_{(24.663,813.87)}$=0.854, η_p^2=0.025, p=0.721). There was no significant group effect ($F_{(2,66)}$=0.13, η_p^2=0.004, p=0.878). These results suggest that prefrontal stimulation prior to MSL did not influence performance accuracy during initial training.

Effect of prefrontal TBS on corticospinal excitability

MEP values did not differ among groups ($F_{(1,57)}$=0.65, η_p^2=0.022, p=0.526) and showed no timepoint by group interaction ($F_{(2,57)}$=0.212, η_p^2=0.007, p=0.81). However, we observed a main effect of timepoint ($F_{(1,57)}$=13.217, η_p^2=0.188, p=0.001) driven by higher MEPs post-TBS compared to pre-TBS (see Supplemental Figure S1).

Supplemental Tables

Supplemental Table S1. Participant characteristics and Sleep/Vigilance scores

	Control group	cTBS group	iTBS group	Statistical analyses
1. Participant characteristics (Main effect of group for statistical analyses)				
N (female)	21 (14)	24 (16)	24 (16)	$\chi^2_{(2)}$=0, *p*=1
Age (years)	23.19 ± 2.96	23.5±2.43	23.58±2.24	$F_{(2,66)}$=0.15 , *p*=0.87
Edinburgh Handedness[4]	86.67±12.08	82.92±16.28	84.79±14.10	$F_{(2,66)}$=0.38, *p*=0.68
Epworth Sleepiness Scale[5]	6.33±3.37	6.38±3.41	7.29±3.5	$F_{(2,66)}$=0.59, *p*=0.56
PSQI[6]	2.48±1.25	2.46±1.285	2.17±1.2	$F_{(2,66)}$=0.46, *p*=0.64
Chronoscore (CRQ)[a] [7]	48.95 ± 7.8	51.13 ± 6.17	51 ± 8.66	$F_{(2,64)}$=0.55, *p*=0.58
Beck Depression Scale[8]	3.14 ± 2.59	3.25 ± 3.6	2.17 ± 3.03	$F_{(2,66)}$=0.86, *p*=0.43
Beck Anxiety Scale[9]	2.62 ± 2.54	2.46 ± 1.64	2.83 ± 3.27	$F_{(2,66)}$=0.13, *p*=0.88
2. Sleep/Vigilance scores				
Sleep duration (h)[b]				Main effect of group: $F_{(2,66)}$=0.98, *p*=0.382
Mean (3 nights)	8.76±1.12	8.42 ± 1.01	8.62 ± 1.04	Main effect of night: $F_{(2,132)}$=2.183, *p*=0.12
Night 1	9.05±1.19	8.32 ± 1.03	8.52 ± 1.17	Night x group interaction: $F_{(4,132)}$=0.91, *p*=0.14
Night 2	8.81±1.12	8.52 ± 0.99	8.84 ± 0.97	
Night 3	8.42±1	8.36 ± 1	8.49 ± 0.97	
St. Mary's Sleep quality[10]				Main effect of group: $F_{(2,66)}$=0.59, *p*=0.56
Night 3	4.14±0.66	3.92±0.83	4±0.59	
Psychomotor vigilance task (s)[11]				Main effect of group: $F_{(2,66)}$=1.56, *p*=0.22
Training	0.29±0.02	0.28±0.02	0.28±0.03	
Stanford sleepiness score[c] [12]				Main effect of group: $F_{(2,64)}$=0.026, *p*=0.98
Training	1.93 ±0.68	1.71±0.61	1.85 ±0.8	

Values are means ± standard deviation. p values are based on one-way ANOVAs with the between-subject factor group (3) and if applicable sessions/nights as within-subject factor. PSQI: Pittsburgh Sleep Quality Index, CRQ: Circadian Rhythm Questionnaire. [a]Chronoscores could not be determined for 2 participants (1 control, 1 iTBS) due to one missing answer each. None of the participants were categorized as extreme morning or evening types.

[b]Sleep duration was assessed based on actiwatch and sleep diary data. Night 1 corresponds to the night 3 days before the experiment.

[c]Stanford sleepiness scores are missing for 2 participants (1 iTBS, 1 control).

Supplemental Table S2. Distribution of the different transitions used in the micro-computations

Transition	4-7	7-3	3-8	8-6	6-2	2-5	5-1	1-4
Mean across groups	47.03	41.39	40.48	38.03	39.46	38.99	40.14	34.48
Mean cTBS	46.46	41.46	40.00	37.75	38.75	39.67	40.46	35.46
Mean iTBS	47.13	41.46	41.08	38.17	40.29	38.42	39.58	33.88
Mean control	47.57	41.24	40.33	38.19	39.99	38.86	40.43	34.05

Values are mean number of transitions per type included in the micro-computation. A two-way repeated-measures ANOVA with transitions (8) as within-subject factor and group (3: cTBS, iTBS, control) as between-subject factor revealed a significant main effect of transition ($F_{(2.633,173.762)}$=45.955, p<0.001), with the transitions early in the sequence - as compared to later in the sequence - contributing more to the calculation of the micro-online and -offline gains. This is in line with the instructions provided to the participants stating that, in case of error, they must start the sequence over. Importantly, there was no significant transition by group interaction ($F_{(5.266,173.762)}$=0.488, p=0.794) or group effect ($F_{(2,66)}$=0.516, p=0.6). Therefore, the heterogenous distribution of the transitions is unlikely to influence the comparisons at the group level.

Supplemental Table S3. Coordinates of areas of interest used for spherical small volume corrections for the main results and for the supplemental results

Area	x mm	y mm	z mm	Reference
HIPPOCAMPUS				
Posterior Hippocampus	±24	-34	2	[13]
Hippocampus	±34	-10	-20	[14]
STRIATUM				
Caudate	±9	15	-3	[15]
Caudate	±15	12	12	[15]
Globus Pallidus	±12	2	0	[16]
TMS target				
DLPFC	-30	22	48	[17]

Coordinates in MNI space. DLPFC: dorsolateral prefrontal cortex, MNI: Montreal Neurological Institute.

Supplemental Table S4. Behavioral results of processes at the micro timescale – pairwise group comparisons (*t* tests)

	cTBS vs. control	iTBS vs. control	cTBS vs. iTBS
micro-offline gains	$t_{(32.390)}$=-2.298, d=0.708, *p*=0.028	$t_{(43)}$=-1.517, d=-0.453, *p*=0.137	$t_{(46)}$=0-.781, d=0-.225, *p*=.439
micro-online gains	$t_{(43)}$=2.348, d=0.702, *p*=0.024	$t_{(43)}$=1.368, d=0.409, *p*=0.178	$t_{(46)}$=0.973, d=0.281, *p*=0.336
overall learning	$t_{(43)}$=0.160, d=0.048, *p*=0.873	$t_{(43)}$=-0.718, d=-0.215, *p*=0.476	$t_{(46)}$=0.855, d=0.247, *p*=0.397

Supplemental Table S5. Functional imaging results of activation-based contrasts – pairwise group comparisons (*t* tests)

Area	x	y	z	k	Z	p_{FWEsvc}
Main effect of practice						
[cTBS-control]						
Hippocampus	-30	-10	-26	48	3.1	0.021*
Caudate	-8	16	4	63	2.99	0.028
[iTBS-control]						
Hippocampus	-28	-10	-26	111	3.5	0.007*
Caudate	-10	16	4	4654	3.35	0.01*
[control-cTBS] | [control-iTBS] | [cTBS-iTBS] | [iTBS-cTBS]						
No significant responses in the ROIs						

Asterisk (*) indicates significance at p<0.05 after Holm-Bonferroni correction for multiple comparison. Statistics were extracted from regions of interest (ROI) without applying anatomical masks.

Supplemental Table S6. Functional imaging results of persistence of task-related brain patterns into inter-practice rest intervals – exploratory pairwise group comparisons (*t* tests) following group effects (caudate nucleus: $F_{(2,66)}$=1.811, η_p^2=0.052, *p*=0.171; hippocampus: $F_{(2,66)}$=1.1, η_p^2=0.032, *p*=0.339; thalamus: $F_{(2,66)}$=0.82, η_p^2=0.024, *p*=0.445).

	control vs. cTBS (one-sided *t* test)	control vs. iTBS (one-sided *t* test)	cTBS vs. iTBS (2-sided *t* test)
caudate nucleus	$t_{(43)}$=1.582, d=-0.473, *p*=0.061	$t_{(43)}$=1.734, d=-0.518, *p*=0.045	$t_{(46)}$=0.255, d=-0.074, *p*=0.8
hippocampus	$t_{(43)}$=1.352, d=-0.404, *p*=0.092	$t_{(43)}$=1.266, d=-.378, *p*=.106	$t_{(46)}$=0.021, d=-0.006, *p*=0.984
thalamus	$t_{(43)}$=0.656, d=-0.196, *p*=0.258	$t_{(43)}$=1.233, d=-.366, *p*=.114	$t_{(46)}$=0.676, d=0.195, *p*=0.502

Supplemental Table S7. Group pair comparisons regarding the relationship between brain activity and pattern persistence as well as micro-offline gains and pattern persistence

	cTBS	iTBS	active	control	cTBS vs. iTBS	cTBS vs. control	iTBS vs. control
correlation between brain activity (see Table 1.1 of main text) and MVCS pattern persistence							
caudate nucleus	r=-0.089; p=0.679	r=-0.168; p=0.434	r=-0.137; p=0.354	r=-0.266; p=0.243	χ^2=0.07, p=0.795	χ^2=0.33, p=0.568	χ^2=0.10, p=0.749
hippocampus	r=0.247; p=0.245	r=-0.074; p=0.731	r=0.049; p=0.74	r=-0.56; p=0.008	χ^2=1.12, p=0.29	χ^2=7.59, p=0.006	χ^2=3.03, p=0.082
correlation between micro-offline gains and MVCS pattern persistence							
caudate nucleus	r=-0.356; p=0.087	r=0.108; p=0.614	r=-0.081; p=0.585	r=-0.063; p=0.787	χ^2=2.4, p=0.119	χ^2=0.93, p=0.336	χ^2=0.29, p=0.593
hippocampus	r=-0.145; p=0.499	r=-0.029; p=0.892	r=-0.074; p=0.617	r=-0.032; p=0.89	χ^2=0.143, p=0.705	χ^2=0.126, p=0.723	χ^2=0.00009, p=0.993
thalamus	r=-0.225; p=0.291	r=0.178; p=0.406	r=0.013; p=0.932	r=0.165; p=0.474	χ^2=1.76, p=0.185	χ^2=1.52, p=0.218	χ^2=0.002, p=0.965

MVCS: multivoxel correlation structure.

Supplemental Table S8. Functional imaging results of the regression analyses between task-related activity maps (main effect of practice) and the sum of micro-offline gains during initial MSL

Area	x	y	z	k	Z	p_{FWEsvc}
Pairwise group comparisons (*t* tests)						
[iTBS-control]						
Hippocampus	26	-30	-6	3	2.77	0.048*
[control-iTBS]||[control-cTBS]||[cTBS-control]||[iTBS-cTBS]||[cTBS-iTBS]						
No significant responses						

Asterisk (*) indicates significance at p<0.05 after Holm-Bonferroni correction for multiple comparison.

Supplemental Figures

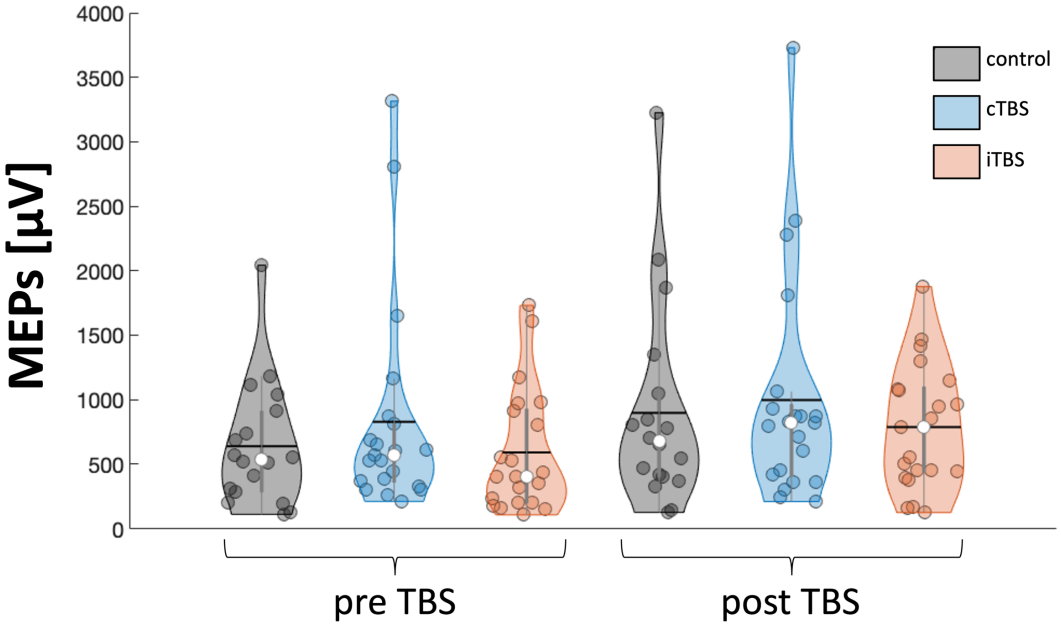

Supplemental Figure S1. MEP values. Raw MEP values increased from pre- to post-TBS similarly in all three groups. Colored circles represent individual data, jittered in arbitrary distances on the x-axis within the respective violin plot to increase perceptibility. Black horizontal lines represent means and white circles represent medians. The shape of the violin plots depicts the distribution of the data and grey vertical lines represent quartiles. MEPs: motor evoked potentials, TBS: theta-burst stimulation, c: continuous, i: intermittent.

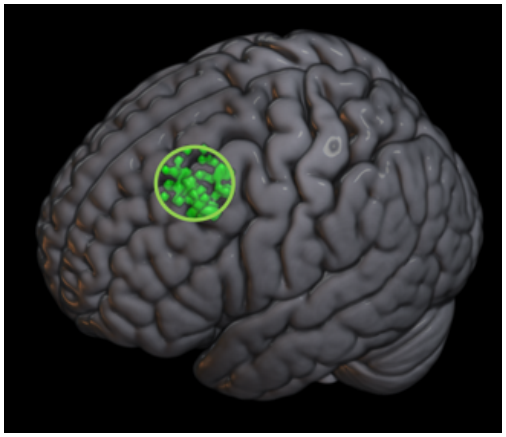

Supplemental Figure S2. Individual DLPFC peaks depicted as 2-mm radius spheres centered on the individually defined coordinates showing maximal connectivity with both the striatum and the hippocampus identified with the targeting pipeline described in[17]. The 15-mm radius search sphere around the group DLPFC target used for the individual targeting pipeline is depicted by the green circle. Results showed significant conjunction peaks within the DLPFC sphere for each individual included in this study.

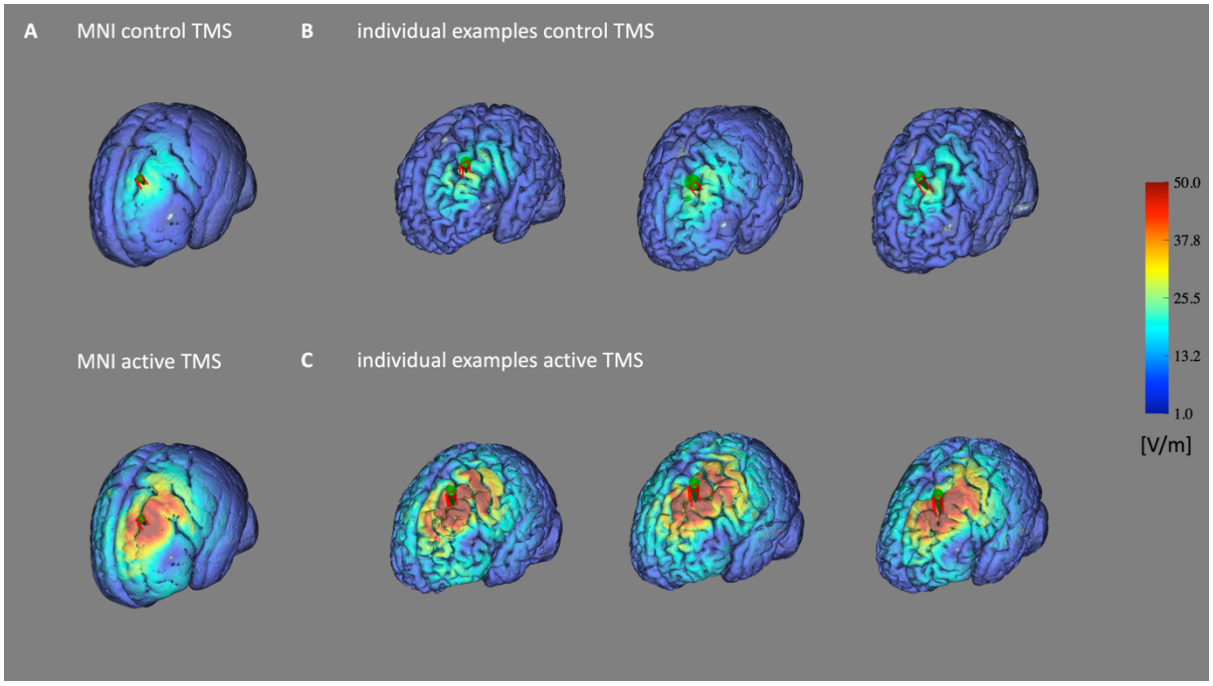

Supplemental Figure S3. Simulated e-fields using 14 000 000 A/s as dI/dt for the control TMS and 31 500 000 A/s as dI/dt for the active TMS on (A) the MNI template, (B) three exemplary individuals from the control TMS group and (C) three exemplary individuals from the active TMS group. The DLPFC target is depicted with the green cone and red cuboid as provided by the Brainsight software.

Supplemental References

1. Nissen, M. J. & Bullemer, P. Attentional requirements of learning: Evidence from performance measures. *Cognit. Psychol.* **19**, 1–32 (1987).
2. Tambini, A., Nee, D. E. & D'Esposito, M. Hippocampal-targeted Theta-burst Stimulation Enhances Associative Memory Formation. *J. Cogn. Neurosci.* **30**, 1452–1472 (2018).
3. van Polanen, V., Rens, G. & Davare, M. The role of the anterior intraparietal sulcus and the lateral occipital cortex in fingertip force scaling and weight perception during object lifting. *J. Neurophysiol.* (2020) doi:10.1152/jn.00771.2019.
4. Oldfield, R. C. The assessment and analysis of handedness: The Edinburgh inventory. *Neuropsychologia* **9**, 97–113 (1971).
5. Johns, M. W. A new method for measuring daytime sleepiness: the Epworth sleepiness scale. *Sleep* **14**, 540–545 (1991).
6. Buysse, D. J., Reynolds, C. F., Monk, T. H., Berman, S. R. & Kupfer, D. J. The Pittsburgh sleep quality index: A new instrument for psychiatric practice and research. *Psychiatry Res.* **28**, 193–213 (1989).
7. Horne, J. A. & Ostberg, O. A self-assessment questionnaire to determine morningness-eveningness in human circadian rhythms. *Int. J. Chronobiol.* **4**, 97–110 (1976).
8. Beck, A. T., Ward, C. H., Mendelson, M., Mock, J. & Erbaugh, J. An Inventory for Measuring Depression. *Arch. Gen. Psychiatry* **4**, 561–571 (1961).
9. Beck, A. T., Epstein, N., Brown, G. & Steer, R. A. An Inventory for Measuring Clinical Anxiety: Psychometric Properties. *J. Consult. Clin. Psychol.* **56**, 893–897 (1988).
10. Ellis, B. *et al.* The St. Mary's Hospital Sleep Questionnaire: A Study of Reliability. *SLEEP* **4**, 93–97 (1981).

11. Dinges, D. F. & Powell, J. W. Microcomputer analyses of performance on a portable, simple visual RT task during sustained operations. *Behav. Res. Methods Instrum. Comput.* **17**, 652–655 (1985).
12. Maclean, A. W., Fekken, G. C., Saskin, P. & Knowles, J. B. Psychometric evaluation of the Stanford Sleepiness Scale. *J. Sleep Res.* **1**, 35–39 (1992).
13. Albouy, G. *et al.* Both the Hippocampus and Striatum Are Involved in Consolidation of Motor Sequence Memory. *Neuron* **58**, 261–272 (2008).
14. Albouy, G. *et al.* Maintaining vs. enhancing motor sequence memories: Respective roles of striatal and hippocampal systems. *NeuroImage* **108**, 423–434 (2015).
15. Schendan, H. E., Searl, M. M., Melrose, R. J. & Stern, C. E. An fMRI study of the role of the medial temporal lobe in implicit and explicit sequence learning. *Neuron* **37**, 1013–1025 (2003).
16. Lehéricy, S. *et al.* Motor control in basal ganglia circuits using fMRI and brain atlas approaches. *Cereb. Cortex* **16**, 149–161 (2006).
17. Gann, M. A. *et al.* Hippocampal and striatal responses during motor learning are modulated by prefrontal cortex stimulation. *NeuroImage* **237**, 118158 (2021).
18. Tzourio-Mazoyer, N, Landeau, B, Papathanassiou, D, Crivello, F, Etard, O, Delcroix, N, Mazoyer, B, Joliot, M, 2002. Automated anatomical labeling of activations in SPM using a macroscopic anatomical parcellation of the MNI MRI single-subject brain. Neuroimage 15, 273–289.
19. Nichols, N. http://www2.warwick.ac.uk/fac/sci/statistics/staff/academic-research/nichols/scripts/fsl/.